

Complete and Incomplete Wetting of Ferrite Grain Boundaries by Austenite in the Low-Alloyed Ferritic Steel

B.B. Straumal, Y.O. Kucheev, L.I. Efron, A.L. Petelin, J. Dutta Majumdar, and I. Manna

(Submitted October 30, 2011; in revised form December 19, 2011)

Low-carbon low-alloyed ferritic steels are the main material for the production of high-strength pipes for the transportation of oil and gas. The formation of brittle carbide network during the lifetime of a pipeline could be a reason for a catastrophic failure. Among other reasons, it can be controlled by the morphology of grain boundary (GB) carbides. The microstructure of a low-alloyed ferritic steel containing 0.09 at.% C and small amounts of Si, Mn, Nb, Cu, Al, Ni, and Cr was studied between 300 and 900 °C. The samples were annealed very long time (700 to 4000 h) in order to produce the equilibrium morphology of phases. The $(\alpha\text{-Fe})/(\alpha\text{-Fe})$ GBs can be either completely or incompletely wetted (covered) by the $\gamma\text{-Fe}$ (austenite) above the temperature of eutectoid transition. The portion of $(\alpha\text{-Fe})/(\alpha\text{-Fe})$ GBs completely wetted by $\gamma\text{-Fe}$ is around 90% and does not change much between 750 and 900 °C. The $(\alpha\text{-Fe})/(\alpha\text{-Fe})$ GBs can be either completely or incompletely wetted (covered) by the Fe_3C (cementite) below the temperature of eutectoid transition. The portion of $(\alpha\text{-Fe})/(\alpha\text{-Fe})$ GBs completely wetted by Fe_3C changes below 680 °C between 67 and 77%. The formation of the network of brittle cementite layers between ductile ferrite grains can explain the catastrophic failure of gas- and oil-pipelines after a certain lifetime.

Keywords failure of pipelines, ferritic steels, grain boundaries, low-alloyed steels, wetting

1. Introduction

Low-carbon low-alloyed ferritic steels are nowadays the main material for the production of high-strength pipes for the transportation of oil and gas. One of the important problems of these steels is the so-called stress-corrosion cracking (Ref 1-5). This failure mode is mainly intergranular. Among other

This article is an invited submission to JMEP selected from presentations at the Symposia “Wetting, soldering and brazing” and “Diffusion bonding and characterization” belonging to the Topic “Joining” at the European Congress and Exhibition on Advanced Materials and Processes (EUROMAT 2011), held September 12-15, 2011, in Montpellier, France, and has been expanded from the original presentation.

B.B. Straumal, Institute of Solid State Physics, Russian Academy of Sciences, Chernogolovka, Russia 142432; National University of Science and Technology «MISiS», Leninsky Prospect 4, Moscow, Russia 119991; Institut für Nanotechnologie, Karlsruher Institut für Technologie (KIT), Hermann-von-Helmholtz-Platz 1, 76344 Eggenstein-Leopoldshafen, Germany; **Y.O. Kucheev**, Institute of Solid State Physics, Russian Academy of Sciences, Chernogolovka, Russia 142432; National University of Science and Technology «MISiS», Leninsky Prospect 4, Moscow, Russia 119991; **L.I. Efron**, United Metallurgical Company, Volgogradskii Prosp. 2, Moscow, Russia 109316; **A.L. Petelin**, National University of Science and Technology «MISiS», Leninsky Prospect 4, Moscow, Russia 119991; **J. Dutta Majumdar**, Metallurgical and Materials Engineering Department, Indian Institute of Technology, Kharagpur, Kharagpur 721302 West Bengal, India; and **I. Manna**, Central Glass and Ceramic Research Institute, 196 Raja S C Mullick Road, Kolkata 700032, India. Contact e-mail: straumal@mf.mpg.de.

reasons, it can be controlled by the morphology of grain boundary (GB) carbides. The carbides can either form the discontinuous array of isolated lenticular particles or the interconnected network of continuous GB layers. Such continuous carbide network is very brittle. The formation of brittle carbide network during the lifetime of a pipeline could be a reason for a catastrophic pipeline failure.

The morphology of second solid phase γ in a GB of a first solid phase α depends on the ratio of the GB energy $\sigma_{\alpha\alpha}$ and the energy $\sigma_{\alpha\gamma}$ of an interphase boundary between α and phases γ . If the GB energy $\sigma_{\alpha\alpha}$ is lower than that of two α/γ interfaces $2\sigma_{\alpha\gamma}$, the particles of a γ -phase are lenticular and form a certain finite contact angle along the triple line of a contact between the α/α GB and the α/γ interface. If the GB energy $\sigma_{\alpha\alpha}$ is higher than that of two α/γ interfaces $2\sigma_{\alpha\gamma}$, the γ -phase forms the continuous GB layer separating both α -grains from each other. In this case the contact angle along the triple line of a contact between the α/α GB and the α/γ interface formally equals zero.

These two possibilities are similar to the wetting of a surface by a liquid phase (melt). If a liquid spreads on the surface, one can speak about full (or complete) wetting. The contact angle between liquid and solid in this case is zero. If a liquid droplet does not spread and forms a finite contact angle, it is a partial (or incomplete) wetting. Cahn (Ref 6) and Ebner and Saam (Ref 7) first assumed that the (reversible) transition from incomplete to complete wetting can proceed with increasing temperature. Such transition has been observed for GBs in polycrystalline samples of Zn-Sn, Zn-Sn-Pb, Ag-Pb (Ref 8, 9), Zn-Sn, Al-Cd, Al-In, Al-Pb (Ref 10), W-Ni, W-Cu, W-Fe, Mo-Ni, Mo-Cu, Mo-Fe (Ref 11). The exact measurements of the temperature dependence for the GB contact angle with the melt were made using the individual GBs in the specially grown bicrystals in the Cu-In (Ref 12), Al-Sn (Ref 13), Zn-Sn (Ref 14), Al-Zn (Ref 15), Sn-Bi (Ref 16), In-Sn (Ref 17), Zn-Sn, and Zn-In (Ref 18) systems. It is rather easy to investigate the GB wetting by a liquid phase (melt) since the

equilibrium can be reached quite quickly, just in few minutes. If the wetting phase is solid, the equilibration is very slow and can take months. Nevertheless, the GB wetting by a second solid phase has been observed and successfully investigated in the Zn-Al (Ref 19), Al-Zn (Ref 20), Al-Mg (Ref 21), and Co-Cu (Ref 22) alloys.

The goal of this work is to experimentally measure the equilibrium amount of ferrite GBs completely wetted (covered) by the austenite above the temperature of eutectoid transformation or by the cementite below this temperature. For this purpose, the low-carbon steel alloyed with small amounts of Si, Mn, Ti, Nb, etc., has been chosen. This composition is typical for steels used in the production of gas- and oil-pipelines.

2. Experimental

The low-alloyed ferritic steel (composition given in Table 1) was prepared of pure 3 N components by the vacuum induction melting. The amount of components other than carbon is low and is below the solubility limit in ferrite (Ref 23). The $10 \times 10 \times 10$ mm samples were cut from the ingots and sealed into evacuated silica ampoules with a residual pressure of approximately 4×10^{-4} Pa at room temperature. Samples were annealed at temperatures between 300 °C (4000 h) and 900 °C (700 h) and then quenched in water. The long annealing duration permitted to reach the equilibrium morphology of GB layers. The annealing temperatures and durations are given in Table 2. The accuracy of the annealing temperature was ± 2 °C. The annealing points were in the ferrite (α -Fe) + austenite (γ -Fe) two-phase area (above cementite \leftrightarrow austenite transition temperature) and in the ferrite (α -Fe) + cementite (Fe_3C) below cementite \leftrightarrow austenite transition temperature. The cementite \leftrightarrow austenite transition proceeds in the binary Fe-C alloys at 738 °C (Ref 23). After quenching, samples were embedded in resin and then mechanically ground and polished, using 1 μm diamond paste in the last polishing step, for the metallographic study. The samples were etched few seconds in the 1% HNO_3 ethyl alcohol solution. After etching, samples were investigated by means of the light microscopy, and scanning electron microscopy (SEM). SEM investigations have been carried out in a Tescan Vega TS5130 MM microscope equipped by the LINK energy-dispersive spectrometer produced by Oxford Instruments. Light microscopy has been performed using Neophot-32 light microscope equipped with 10 Mpix Canon Digital Rebel XT camera. Typical micrographs obtained by SEM are shown in Fig. 2. A quantitative analysis of the wetting transition was performed adopting the following criterion: every (α -Fe)/(α -Fe) GB was considered to be completely wetted only when a layer of γ -Fe- or Fe_3C -rich film had covered the whole GB (shown by arrows with symbol “C”, Fig. 2b). If such a layer appeared to be interrupted, the GB was regarded as incompletely (shown by arrows with

symbol “I”, Fig. 2b) wetted. At least 100 GBs were analyzed at each temperature.

3. Results and Discussion

In Fig. 1 the SEM micrographs of typical structures for the alloys above (Fig. 2a, 800 °C) and below (Fig. 2b, 700 °C) eutectoid transformation are shown. The α -Fe grains (matrix) appear dark gray in both cases. The samples annealed between 750 and 900 °C underwent the austenite \rightarrow (ferrite + cementite) transformation by quenching. Therefore, the former austenite grains and GB layers transformed after quenching into the very fine-grained (ferrite + cementite) eutectoid mixture. The former austenite grains and GB layers become very good visible in the SEM micrographs (Fig. 1a) since the 1% HNO_3 etching solution removes the surface layer of ferrite and does not etch cementite. The ferrite in the samples annealed at 680 °C and below is also positioned slightly deeper than the un-etched cementite grains and intergranular layers.

In Fig. 2 the temperature dependence is shown for the portion of ferrite (α -Fe) GBs completely wetted by the cementite (Fe_3C , squares, below 738 °C) or austenite (γ -Fe, circles, above 738 °C) layers. Dotted line shows the cementite \leftrightarrow austenite transition temperature for the binary Fe-C alloys (Ref 23). The majority of the (α -Fe)/(α -Fe) GBs is completely wetted by a second solid phase both below and above cementite \leftrightarrow austenite transition temperature (see microstructures in Fig. 1a and b). Above the eutectoid transformation the (α -Fe)/(α -Fe) GBs are completely wetted by the γ -Fe (austenite) layers. The amount of completely wetted GBs is around 90% and does not change much between 750 and 900 °C (Fig. 2). Below the eutectoid transformation the (α -Fe)/(α -Fe) GBs are completely wetted by the Fe_3C (cementite) layers. The amount of completely wetted GBs is lower than that in the α -Fe + γ -Fe two-phase area of the Fe-C-X (X are other components, see Table 1). It is around 70-75% between 300 and 680 °C and has a flat minimum at 480 °C. It means that in the studied steel used for the production of gas- and oil-pipelines the cementite should form a network of brittle GB layers close to the equilibrium. In other words, after certain lifetime the danger of catastrophic failure of pipelines can appear. The fine tuning of the steel composition could help to change the surface tension of GBs and interphase boundaries and, in such a way, to exclude the risk of catastrophic failure of gas- and oil-pipelines.

4. Conclusions

1. In the (α -Fe + γ -Fe) two-phase field of the Fe-C-X phase diagram the γ -Fe (austenite) phase can either completely or incompletely wet the (α -Fe)/(α -Fe) GBs.

Table 1 Composition of the studied alloy in at.%, Fe-balance

Element at.%	C	Si	Mn	P	S	Cr	Ni	Cu	Al	Ti	Nb	N
	0.09	0.36	1.33	0.009	0.002	0.03	0.02	0.03	0.03	0.015	0.054	0.007

Table 2 Annealing temperature (T , °C) and duration (t , 10^3 h)

T	300	400	450	480	520	600	660	680	750	775	800	825	875	900
t	4.0	3.5	3.0	2.5	2.0	1.5	1.4	1.2	1.2	1.0	1.0	0.9	0.8	0.7

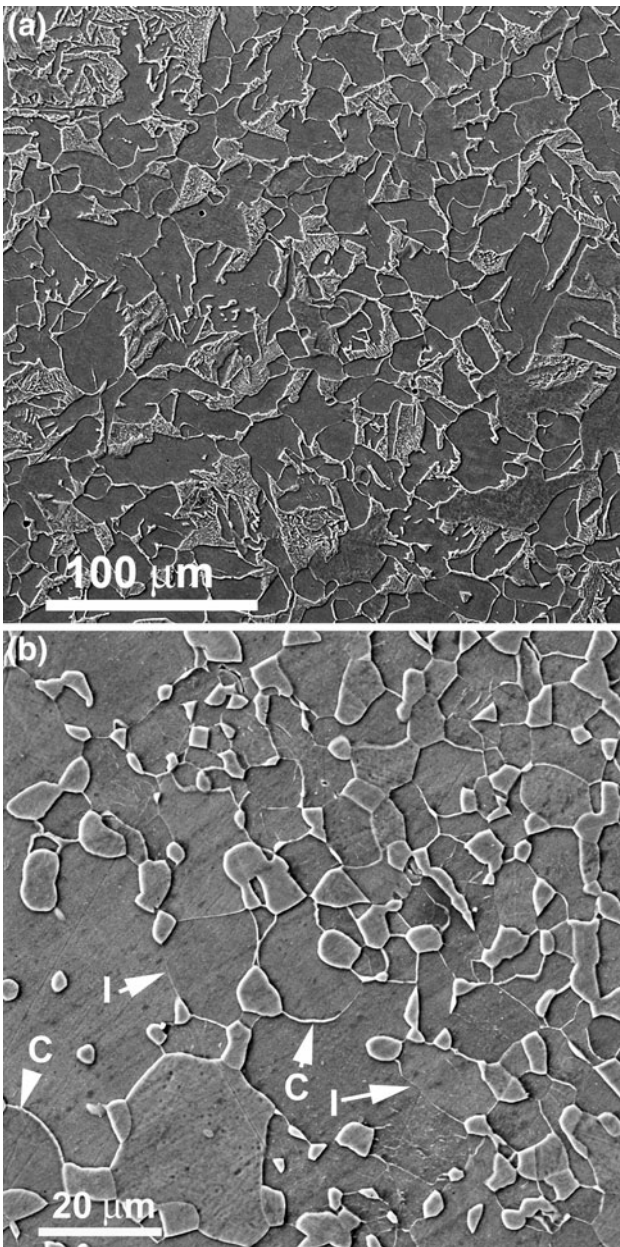


Fig. 1 SEM micrographs of the steel samples annealed (a) at 800 °C in the ferrite (α -Fe) + austenite (γ -Fe) area of the phase diagram and (b) at 660 °C in the ferrite (α -Fe) + cementite (Fe_3C) area of the phase diagram. The arrows mark ferrite GBs completely (C) and incompletely (I) wetted by the cementite layers

2. In the (α -Fe + Fe_3C) two-phase field of the Fe-C-X phase diagram the Fe_3C (cementite) phase can either completely or incompletely wet the (α -Fe)/(α -Fe) GBs.
3. The portion of (α -Fe)/(α -Fe) GBs completely wetted by γ -Fe is around 90% and does not change much between 750 and 900 °C.
4. The portion of (α -Fe)/(α -Fe) GBs completely wetted by Fe_3C changes below 680 °C between 67 and 77%.
5. The formation of the network of brittle cementite layers between ductile ferrite grains can explain the catastrophic failure of gas- and oil-pipelines after a certain lifetime.

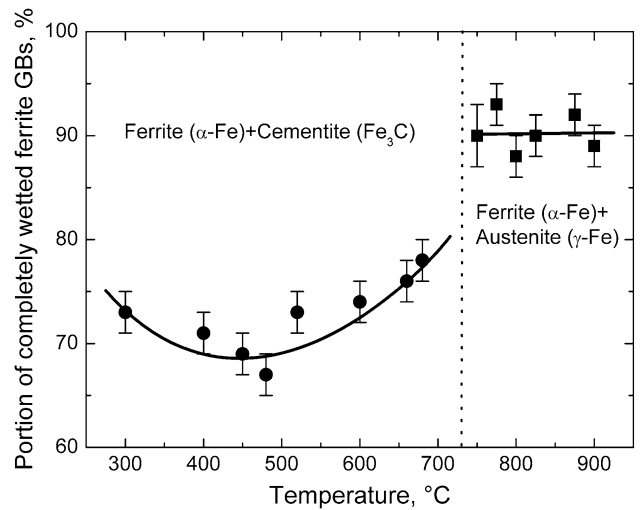


Fig. 2 Temperature dependence for the portion of ferrite (α -Fe) GBs completely wetted by the cementite (Fe_3C , squares, below 738 °C) or austenite (γ -Fe, circles, above 738 °C) layers. Dotted line shows the cementite \leftrightarrow austenite transition temperature for the binary Fe-C alloys (Ref 23)

Acknowledgments

The authors thank for the financial support the Programme of Creation and Development of the National University of Science and Technology “MISI”, Russian Foundation of Basic Research (contracts 09-03-00784, 08-08-91302) and Department of Science and Technology of the Government of India (contract RUSP-873).

References

1. H. Nykyforchyn, E. Lunarska, O.T. Tsyulnyk, K. Nikiforov, M.E. Genarro, and G. Gabetta, Environmentally Assisted “In-Bulk” Steel degradation of Long Term Service Gas Trunkline, *Eng. Fail. Anal.*, 2010, **17**, p 624–632
2. YuP Surkov, V.G. Rybalko, D.V. Novgorodov, AYu Surkov, R.A. Sadrtidinov, and V.B. Geitsan, Estimating the Probability of the Propagation of Stress Corrosion Cracks in Compressor Station Pipelines, *Russ. J. Nondestruct. Test.*, 2010, **46**, p 458–467
3. G.Y. Lee, D. Bae, and S. Park, Assessment of the Crack Growth Characteristics at the Low Corrosion Fatigue Limit of an A106GrB Steel Pipe Weld, *Met. Mater. Int.*, 2010, **16**, p 317–321
4. S.G. Polyakov and A.A. Rybakov, The Main Mechanisms of Stress Corrosion Cracking in Natural Gas Trunk Lines, *Strength Mater.*, 2009, **41**, p 456–463
5. J.Y. Koo, M.J. Luton, N.V. Bangaru, R.A. Petkovic, D.P. Fairchild, C.W. Petersen, H. Asahi, T. Hara, Y. Terada, M. Sugiyama, H. Tamehiro, Y. Komizo, S. Okaguchi, M. Hamada, A. Yamamoto, and I. Takeuchi, Metallurgical Design of Ultra High-Strength Steels for Gas Pipelines, *Int. J. Offshore Polar Eng.*, 2004, **14**, p 2–10
6. J.W. Cahn, Critical Point Wetting, *J. Chem. Phys.*, 1977, **66**, p 3667–3676
7. C. Ebner and W.F. Saam, New Phase-Transition Phenomena in Thin Argon Films, *Phys. Rev. Lett.*, 1977, **38**, p 1486–1489
8. A. Passerone, N. Eustathopoulos, and P. Desré, Interfacial Tensions in Zn, Zn-Sn and Zn-Sn-Pb Systems, *J. Less-Common Met.*, 1977, **52**, p 37–49
9. A. Passerone, R. Sangiorgi, and N. Eustathopoulos, Interfacial Tensions and Adsorption in the Ag-Pb System, *Scripta Metall.*, 1982, **16**, p 547–550
10. N. Eustathopoulos, Energetics of Solid/Liquid Interfaces of Metals and Alloys, *Int. Met. Rev.*, 1983, **28**, p 189–210
11. B.B. Straumal, *Grain Boundary Phase Transitions*, Nauka Publishers, Moscow, 2003 (in Russian)

12. B. Straumal, T. Muschik, W. Gust, and B. Predel, The Wetting Transition in High and Low Energy Grain Boundaries in the Cu(In) System, *Acta Metall. Mater.*, 1992, **40**, p 939–945
13. B. Straumal, D. Molodov, and W. Gust, Wetting Transition on the Grain Boundaries in Al Contacting with Sn-Rich Melt, *Interface Sci.*, 1995, **3**, p 127–132
14. B. Straumal, W. Gust, and T. Watanabe, Tie Lines of the Grain Boundary Wetting Phase Transition in the Zn-rich Part of the Zn–Sn Phase Diagram, *Mater. Sci. Forum*, 1999, **294–296**, p 411–414
15. B.B. Straumal, A.S. Gornakova, O.A. Kogtenkova, S.G. Protasova, V.G. Sursaeva, and B. Baretzky, Continuous and Discontinuous Grain Boundary Wetting in the Zn–Al System, *Phys. Rev. B*, 2008, **78**, p 054202
16. C.-H. Yeh, L.-S. Chang, and B.B. Straumal, Wetting Transition of Grain Boundaries in the Sn-Rich Part of the Sn–Bi Phase Diagram, *J. Mater. Sci.*, 2011, **46**, p 1557–1562
17. C.-H. Yeh, L.-S. Chang, and B.B. Straumal, Wetting Transition of Grain Boundaries in Tin-Rich Indium-Based Alloys and Its Influence on Electrical Properties, *Mater. Trans.*, 2010, **51**, p 1677–1682
18. A.S. Gornakova, B.B. Straumal, S. Tsurekawa, L.-S. Chang, and A.N. Nekrasov, Grain Boundary Wetting Phase Transformations in the Zn–Sn and Zn–In Systems, *Rev. Adv. Mater. Sci.*, 2009, **21**, p 18–26
19. G.A. López, E.J. Mittemeijer, and B.B. Straumal, Grain Boundary Wetting by a Solid Phase; Microstructural Development in a Zn–5 wt.% Al Alloy, *Acta Mater.*, 2004, **52**, p 4537–4545
20. S.G. Protasova, O.A. Kogtenkova, B.B. Straumal, P. Zięba, and B. Baretzky, Inversed Solid-Phase Grain Boundary Wetting in the Al–Zn System, *J. Mater. Sci.*, 2011, **46**, p 4349–4353
21. B.B. Straumal, B. Baretzky, O.A. Kogtenkova, A.B. Straumal, and A.S. Sidorenko, Wetting of Grain Boundaries in Al by the Solid Al₃Mg₂ Phase, *J. Mater. Sci.*, 2010, **45**, p 2057–2061
22. B.B. Straumal, O.A. Kogtenkova, A.B. Straumal, YuO Kuchyeyev, and B. Baretzky, Contact Angles by the Solid-Phase Grain Boundary Wetting in the Co–Cu System, *J. Mater. Sci.*, 2010, **45**, p 4271–4275
23. T.B. Massalski, Ed., *Binary Alloy Phase Diagrams*, 2nd ed., ASM International, Materials Park, OH, 1990